Electrical Power and Energy Systems 132 (2021) 107214

Contents lists available at ScienceDirect

International Journal of Electrical Power and Energy Systems

journal homepage: www.elsevier.com/locate/ijepes

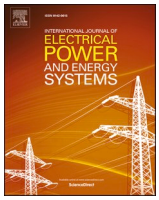

A two-stage resilience improvement planning for power distribution systems against hurricanes

Mostafa Ghasemi [a,b], Ahad Kazemi [a,*], Ettore Bompard [b], Farrokh Aminifar [c]

[a] Centre of Excellence for Power System Automation and Operation, Department of Electrical Engineering, Iran University of Science and Technology, Tehran, Iran
[b] Dipartimento Energia, Politecnico di Torino, Torino, Italy
[c] Department of Electrical Engineering, Faculty of Engineering, University of Tehran, Tehran, Iran

ARTICLE INFO

Keywords:
Distribution system planning
Resilience analysis
Stochastic optimization
Uncertainty

ABSTRACT

This paper presents a novel planning strategy for distribution system planners (DSPs) to enhance the resilience of distribution systems confronting emergencies. The problem is formulated as a two-stage stochastic programming model under emergency and normal scenarios. The decisions on line hardening, distributed generation (DG) placement, mobile emergency generators (MEG) allocation, and tie switch placement are made in the first stage to maximize the system resilience. In the second stage, the operation costs of the system pertaining to the DSP power purchase from the upstream network, DG power production, and forced load shedding in emergency conditions are minimized to achieve a techno-economic compromise of investment costs and enhanced operation/resilience benefits over both planning and operation scales. Since access to dependable distribution functions for probabilistic approaches is a notable challenge in resilience studies, an uncertainty modeling approach is presented based on the thresholds for the line damage in the worst-case event. The proposed approach can drastically decrease the number of line damage scenarios for resilience studies. The efficiency and effectiveness of the new approach are validated on two distribution system testbeds with 33 and 118 nodes.

1. Introduction

Extreme weather conditions have resulted in long and widespread electricity service interruptions with enormous economic losses in recent years [1]. For example, Hurricanes Harvey and Irma resulted in power interruptions that affected several million customers in Texas and Florida for 14 and 5 days, respectively [2,3]. Unfortunately, the future is even hazier as more frequent and severe extreme events such as hurricanes and floods are anticipated due to continuing climate change [4]. Accordingly, enhancing the resilience of electricity distribution networks against extreme weather events is sought after by power engineers.

The concept of resilience includes the capability of a system to resist disruptive events and to rapidly recover afterward [5]. The majority of existing studies have focused on the operational measures to quickly recover distribution networks after an extreme weather event [6–8]. However, the resistance and recovery attributes of resilience can be attained and extended only by investment in various sections and components of distribution networks. Generally, upgrading distribution network poles, installing distributed generators (DGs), deploying mobile emergency generators (MEGs), and adding automatic switches are effective planning measures taken by utilities for resilience improvement. Upgrading distribution poles with stronger materials can make them less vulnerable to extreme weather events. DGs can supply on-site power for critical loads and form microgrids to recover loads after an extreme weather event [9–12]. Truck-mounted MEGs, which are extremely flexible resources in emergency conditions, enhance the distribution system resilience with their mobility. Although the operational aspects of MEG deployment for boosting the resilience of distribution systems have been well studied [13–15], its planning with respect to the type, number, and capacity of the required MEGs has poor literature. Remote control switches enable network reconfiguration that can reroute power flow to down sections and, hence, increase the restoration ability of the distribution network [4]. Exploiting these strategies, especially back-up DGs, only for resilience enhancement might be uneconomical due to their considerable installation costs. However, they can be multi-objectively placed in the network where they provide an acceptable economic value during normal operations and effective resilience assistance during emergency conditions.

The problem of resilient distribution system planning is subject to a high level of uncertainty. Robust, information gap decision theory

* Corresponding author.
E-mail address: kazemi@iust.ac.ir (A. Kazemi).

https://doi.org/10.1016/j.ijepes.2021.107214
Received 24 December 2020; Received in revised form 26 April 2021; Accepted 17 May 2021
Available online 26 May 2021

Nomenclature

Indices

d,e,i,j,r	Indices for nodes
k	Index for MEGs
p	Index for the depot of the crew team
s	Index for emergency operation scenarios
t	Index for time
ts	Index for thresholds
w	Index for normal operation scenarios

Sets

B	Set of lines (i,j)
BS	Set of substation node
D	Set of nodes with DG
E	Set of nodes with MEG
K	Set of MEGs
L	Set of nodes with load
N	Set of all nodes
NW	Set of lines without switch
R	Set of substation nodes
S	Set of emergency scenarios
SW	Set of lines with switch

Parameters

c_d^{dg}	Investment cost ($) for installing a DG at node d
$c_{i,j}^{c}$	Tie-line creation cost ($/km)
$c_{i,j}^{h}$	Investment cost ($) of hardening line (i,j)
c_i^{ls}	Penalty cost ($) for load shedding at node i
c_p^{meg}	Investment cost ($) for allocating a MEG at depot p
$c_{i,j}^{sw}$	Investment cost ($) for installing a remotely controlled tie switch at line (i,j)
C_o^{DG}	Cost ($) of DG operation
C^{sub}	Cost ($) of purchasing power from the upstream network
$LTS_{i,j}$	Length of the tie line (i,j)
M	A sufficiently big number
N_{DG}	Allowed number of newly installed DGs
$N_{pole,i,j}$	Number of poles in line (i,j)
Nts	Number of thresholds
N_w	Number of normal scenarios
$p_{i,j}$	Failure probability of line (i,j)
p_{pole}	Failure probability of pole
P_d^{DGmax}, Q_d^{DGmax}	Maximum active power (kW) and reactive power (kvar) limit of DG at bus d
$P_{i,j}^{max}, Q_{i,j}^{max}$	Active power flow (kW) and reactive power flow (kvar) limits of line (i,j)
$P_{i,t}^{s}, Q_{i,t}^{s}$	Active load (kW) and reactive load (kvar) at node i in scenario s
$P_{i,t}^{w}, Q_{i,t}^{w}$	Active load (kW) and reactive load (kvar) at node i in scenario w
$P_k^{MEGmax}, Q_k^{MEGmax}$	Maximum active power (kW) and reactive power (kvar) limit of MEG k
r	Annual interest rate
$r_{i,j}$	Resistance (pu) of line (i,j)
T_w	Duration of normal scenarios
TH_{ts}	Threshold ts
V_1	Voltage of reference bus (pu)
w_m	Maximum forecast wind power
$x_{i,j}$	Reactance (pu) of line (i,j)
$x_{i,j}^{r_0}$	1 if line (i,j) has an existing switch; 0 otherwise
X_p	Allowed number of MEGs allocated to the depot of crew team p
Y	Planning year horizon
$z_{i,j,t}^{s}$	1 if line (i,j) is damaged based on the threshold in scenario s; 0 otherwise
γ	Capital recovery factor
ε	Voltage deviation tolerance (pu)
π_l	Probability of load scenarios
π_s	Probability of each emergency scenario
π_{ts}^{TH}	Probability of line damage scenarios
ω_1, ω_2	Weighting coefficients

Variables

EC_s	Emergency operation cost ($) in scenario s
IC_{TC}	Investment cost ($)
NC_w	Normal operation cost ($) in scenario w
$P_{e,t}^{MEG,s}, Q_{e,t}^{MEG,s}$	Active power (kW) and reactive power (kvar) output of MEG e in scenario s
$P_{d,t}^{DG,s}, Q_{d,t}^{DG,s}$	Active power (kW) and reactive power (kvar) output of DG d in scenario s
$P_{d,t}^{DG,w}, Q_{d,t}^{DG,w}$	Active power (kW) and reactive power (kvar) output of DG d in scenario w
$P_{i,j,t}^{s}, Q_{i,j,t}^{s}$	Active power flow (kW) and reactive power flow (kvar) of line (i,j) in scenario s
$P_{i,j,t}^{w}, Q_{i,j,t}^{w}$	Active power flow (kW) and reactive power flow (kvar) of line (i,j) in scenario w
$P_{r,t}^{SUB,s}, Q_{r,t}^{SUB,s}$	Power injection from (kW) substation r in scenario s
$P_{r,t}^{SUB,w}, Q_{r,t}^{SUB,w}$	Power injection (kW) from substation r in scenario w
$u_{i,j,t}^{s}$	1 if line (i,j) status is damaged in scenario s; 0 otherwise
$V_{i,t}^{s}$	Voltage (pu) of node i in scenario s
$V_{i,t}^{w}$	Voltage (pu) of node i in scenario w
x_d^{dg}	1 if a DG is installed at node i; 0 otherwise
$x_{i,j}^{h}$	1 if line (i,j) is hardened; 0 otherwise
$x_{i,j}^{r}$	1 if line (i,j) has switch; 0 otherwise
$x_{i,j}^{r_1}$	1 if new switch is added to line (i,j); 0 otherwise
$x_{p,k}$	1 if MEG k is allocated to depot p; 0 otherwise
$y_{p,k,e}^{s}$	1 if MEG k is sent from depot p to node e in scenario s; 0 otherwise
$\alpha_{i,j,t}^{s}$	1 if i is the parent node of j in scenario s; 0 otherwise
$\alpha_{i,j,t}^{w}$	1 if i is the parent node of j in scenario w; 0 otherwise
$\beta_{i,j,t}^{r,s}$	1 if line switch of line (i,j) is closed in scenario s; 0 otherwise
$\rho_{i,t}^{s}$	Load shedding percentage of load i in scenario s

(IGDT), and stochastic optimization frameworks as three types of uncertainty modeling are already utilized to tackle this challenge. In [16], a multi-disaster-scenario distributionally robust planning model was proposed to hedge against two types of natural disaster uncertainties. In this work, a predetermined number of distribution lines were assumed to be damaged by the hurricane. In [17], a tri-level optimization model was presented to solve the grid hardening investment problem based on two alternatives, namely managing vegetation and upgrading distribution poles. However, some important measures such as DGs, MEGs, and automatic tie switches were not included. In [18], a tri-level two-stage robust programming model was proposed to enhance the distribution network resilience through line hardening and forming multiple provisional microgrids. In the master problem, the line hardening strategies were determined, and the subproblem involved finding the impact of the

Table 1
Survey of previous resilience studies in distribution systems.

	Formulation	Power Flow	Resilience measures					Models	Stochastic variables		Operation strategy	
			Hardening	DG	MEG	Switch	Tie-line		Line damage	Load	Emergency	Normal
[5]	MILP	DistFlow						Stochastic	✓		✓	
[16]	MILP	DistFlow	✓	✓				Robust		✓	✓	
[18]	MILP	AC-PF	✓					Robust			✓	
[19]	MINLP	AC-PF	✓	✓				IGDT			✓	
[20]	MILP	AC-PF	✓	✓		✓		Stochastic	✓		✓	
[21]	MILP	DistFlow	✓	✓		✓		Stochastic	✓	✓	✓	
This paper	MILP	Linearized DistFlow	✓	✓	✓	✓	✓	Stochastic	✓	✓	✓	✓

worst contingencies related to the optimal operation of provisional microgrids. This work did not consider the fragility models of distribution network components for the evaluation of contingency probabilities. The calculation of *N-k* contingencies in robust optimization is computationally cumbersome given the increasing size of distribution systems. In [19], a novel strategy based on the IGDT approach was presented for modeling the uncertain characteristics of natural disasters in order to improve the distribution system resilience. This work finds the best DG installation and hardening scheme based on a limited planning budget. However, the IGDT technique can be overly conservative and computationally cumbersome in resilient distribution system planning.

Stochastic programming, as another effective means for uncertainty handling, generates representative scenarios for uncertain parameters. In [20], a two-stage stochastic optimization model was presented for designing resilient distribution networks by deploying various measures such as hardening existing lines, building new lines, adding switches, and installing DGs. This work captured damage scenarios pertaining to natural disasters as stochastic events for evaluating the distribution network performance in the wake of a disaster. In [21], a two-stage stochastic mixed-integer model was proposed to protect distribution networks against extreme weather events. In the first stage, the model identified resilience-oriented design decisions. In the second stage, the system operation cost and the damage repair cost after the event were assessed. In [5], a stochastic programming model was developed for the allocation of the distribution network hardening budget. This work captured the effect of extreme weather events on distribution networks using the Bernoulli distribution. In [22], a novel two-stage stochastic optimization approach was formulated to assess the impacts of investment decisions and uncertainties on the distribution system performance during and after emergency conditions. This work presented a hybrid stochastic process and deterministic causal structure to accommodate the correlations of various uncertainties. In [23], a two-stage stochastic optimization model was proposed to enhance the resilience of the distribution system by using a social welfare index. This work obtained the operation state of the distribution equipment by comparing the failure probability of components with a uniform random number. However, a lack of sufficient information such as a certain distribution function for the line damage scenario is a barrier in real practice. The taxonomy of previous literature in distribution systems is summarized in Table 1, which includes formulation, Power Flow (PF) model, resilience measures, optimization models, and operation strategy.

To fill the gap, this paper proposes a two-stage stochastic mixed-integer linear programming (MILP) model to formulate the resilient distribution system planning problem based on specific thresholds for line damage scenarios in emergency conditions. In this model, the first stage decides about planning measures. The second stage assesses the load shedding penalty cost under an extreme weather event, which is a direct criterion for distribution system resilience enhancement. Since the DG placement problem in distribution networks is necessary during normal operations, the DG operation cost and the cost of purchasing power from the bulk power system are also encompassed in the second stage. Moreover, due to a lack of information such as appropriate distribution functions for probabilistic methods, modeling wind speed as a random variable in resilient distribution system planning is a difficult task. This paper resolves this issue by using a threshold method based on the maximum wind speed. The key contributions and features of the proposed approach are the following:

- A novel linear two-stage stochastic optimization framework is developed for resilient distribution system planning.
- In this framework, the operation strategy of distribution networks is devised for both emergency and normal conditions to achieve a trade-off between the economic value of resources during normal operations and their capability to enhance distribution network resilience in case of emergency operation.
- The uncertainty of line damage is captured based on the maximum wind speed.
- Various facilities, namely line hardening, DG placement, MEG allocation, and tie switch installation, are simultaneously planned for enhancing the resilience of the distribution system.

The rest of the paper is divided into the following sections. Section 2 describes in detail the two-stage stochastic optimization model for resilient distribution system planning and uncertainty modeling of extreme weather events. The simulation data are presented and the results are discussed in Section 3. Finally, the conclusions are drawn in Section 4.

2. The proposed two-stage stochastic optimization formulation

This section builds a two-stage optimization model to optimize investment decisions in the first stage and minimize the operation and curtailment costs associated with normal emergency scenarios in the second stage. The problem of the first stage is a linear integer program, and that of the second stage is a mixed-integer linear program.

2.1. The first-stage problem

The proposed planning model is depicted in Fig. 1 with the relationships between the investment and operation problems. The

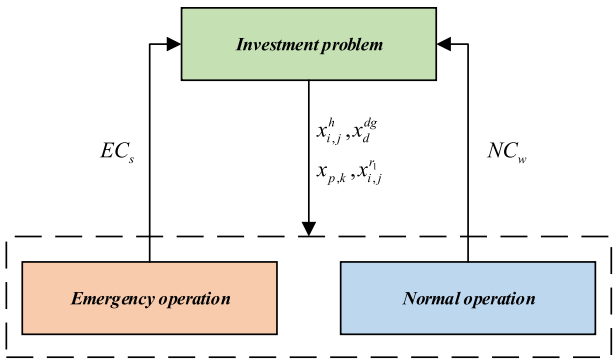

Fig. 1. The proposed planning problem.

objective function of this stage is given as follows:

$$min\ [\gamma IC_{TC} + \omega_1 EC_s + \omega_2 NC_w] \tag{1}$$

$$IC_{TC} = \sum_{(i,j)\in B} x^h_{i,j} c^h_{i,j} + \sum_{d\in D} x^{dg}_d c^{dg}_d + \sum_{(i,j)\in SW} x^{r_1}_{i,j}(c^{sw}_{i,j} + LTS_{i,j} c^c_{i,j}) + \sum_{p\in P}\sum_{k\in K} x_{p,k} c^{meg}_p \tag{2}$$

$$\gamma = \frac{r(1+r)^Y}{(1+r)^Y - 1} \tag{3}$$

$$\sum_{i\in D} x^{dg}_i \leqslant N_{DG} \tag{4}$$

$$\sum_{k\in K} x_{p,k} \leqslant X_p, \forall p \tag{5}$$

$$\sum_{p\in P} x_{p,k} = 1, \forall k \tag{6}$$

$$x^{r_0}_{i,j} + x^{r_1}_{i,j} = x^r_{i,j}, \forall (i,j) \in SW \tag{7}$$

IC_{TC} denotes the first-stage costs including the following: I) cost of hardening existing lines, II) cost of DG installation, III) cost of MEG allocation, and IV) cost of tie switch placement. The cost of tie switch placement consists of two parts, namely the cost of tie switch installation and the cost of tie-line creation. x^h_{ij}, x^{dg}_d, $x^{r_1}_{ij}$ and $x_{p,k}$ are binary variables determining whether line (i,j) is hardened, the DG is installed, a new switch is added to line (i,j), and the MEG is allocated to depot p, respectively. Moreover, EC_s reflects the emergency operation cost, which is the penalty cost of load shedding, and NC_w represents the normal operation cost, which is the cost of DG operation and the cost of purchasing power from the upstream network. ω_1 and ω_2 are the weighting coefficients of the emergency and normal operations, respectively. These coefficients are specified in such a way as to improve resilience. In addition, the total annual capital cost of each strategy is calculated based on the capital recovery factor using (3). Eq. (4) limits the number of back-up DGs that can be installed. The number of MEGs at each crew team depot is restricted by its capacity as in (5). Constraint (6) ensures that each MEG is allocated to only one of the crew team depots. Constraint (7) represents the status of switch installation at line (i,j). $x^{r_1}_{ij}$, as a first stage decision variable, represents whether or not a new switch was added at line (i,j). x^r_{ij}, as a second stage decision variable, indicates whether line (i,j) has a switch or not. If there is a tie switch on line (i,j), adding a new switch is not justified, i.e.,$x^{r_1}_{ij} = 0$ if $x^{r_0}_{ij} = 1$. Otherwise, it can be equipped but depending on the first stage decision $x^{r_1}_{ij}$. Note that $x^{r_0}_{ij}$ is a known parameter.

2.2. Emergency operation in the second-stage problem

If a hurricane occurs, the utility deploys various resilience strategies to limit the damage and economic losses. As a result, the utilities must supply loads based on their priority in emergency operation. The objective function of the utility is given by the following:

$$min\ EC_s = \sum_{s\in S} \pi_s \sum_{t\in T}\sum_{i\in L} \rho^s_{i,t} c^{ls}_i P^s_{i,t} \tag{8}$$

EC_s is the cost of load shedding over a set of emergency scenarios. $\rho^s_{i,t}$ and c^{ls}_i are the load shedding percentage of load i and the penalty cost for load shedding, respectively. π_s is the probability of each emergency scenario. The optimization problem constraints are given in the following in the form of operation restrictions in the case of emergencies.

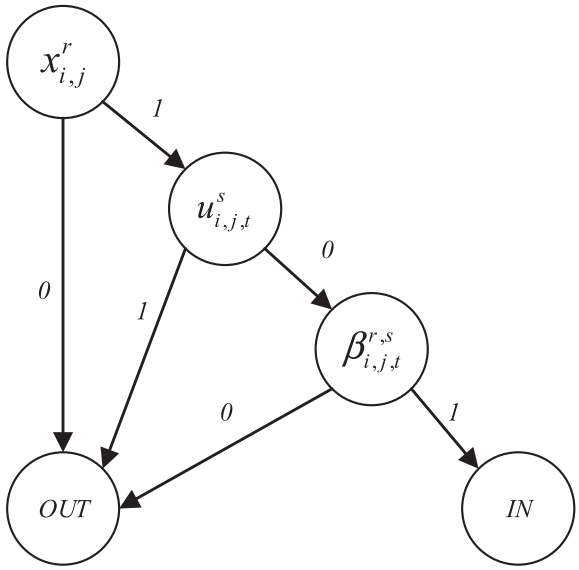

Fig. 2. Distribution line status with tie switch.

(1) Line damage status limit: In this paper, we assumed that hardened distribution lines would not be damaged in future extreme weather events. However, a few resilience studies consider the fact that the hardened distribution lines are still vulnerable to damages with lower probabilities [17,24]. Constraint (9) links the functional status of distribution lines with their damage status and the hardening strategy.

$$u^s_{i,j,t} = (1 - x^h_{ij}) \times z^s_{i,j,t}, \forall (i,j) \in B, t \tag{9}$$

Based on (9), first, we need to sample $z^s_{i,j,t}$ (explained in Section 2.4) for all distribution lines in the scenario generation phase. Then, the damage status of a distribution line $u^s_{i,j,t}$ is considered based on the first-stage decision x^h_{ij} and the uncertainty realization of line outage$z^s_{i,j,t}$.

(2) Line flow limits: The following constraints provide the full set of power flow limitations.

$$\beta^{r,s}_{i,j,t} \leqslant x^r_{i,j}, \forall (i,j) \in SW, t \tag{10}$$

$$\beta^{r,s}_{i,j,t} + u^s_{i,j,t} \leqslant 1, \forall (i,j) \in SW, t \tag{11}$$

$$-\beta^{r,s}_{i,j,t} P^{max}_{ij} - (1 - x^r_{ij}) M \leqslant P^s_{i,j,t} \leqslant \beta^{r,s}_{i,j,t} P^{max}_{ij} + (1 - x^r_{ij}) M, \forall (i,j) \in SW, t \tag{12}$$

$$-\beta^{r,s}_{i,j,t} Q^{max}_{ij} - (1 - x^r_{ij}) M \leqslant Q^s_{i,j,t} \leqslant \beta^{r,s}_{i,j,t} Q^{max}_{ij} + (1 - x^r_{ij}) M, \forall (i,j) \in SW, t \tag{13}$$

$$-x^r_{ij} M \leqslant P^s_{i,j,t} \leqslant x^r_{ij} M, \forall (i,j) \in SW, t \tag{14}$$

$$-x^r_{ij} M \leqslant Q^s_{i,j,t} \leqslant x^r_{ij} M, \forall (i,j) \in SW, t \tag{15}$$

$$-(1 - u^s_{i,j,t}) P^{max}_{ij} \leqslant P^s_{i,j,t} \leqslant (1 - u^s_{i,j,t}) P^{max}_{ij}, \forall (i,j) \in NW, t \tag{16}$$

$$-(1 - u^s_{i,j,t}) Q^{max}_{ij} \leqslant Q^s_{i,j,t} \leqslant (1 - u^s_{i,j,t}) Q^{max}_{ij}, \forall (i,j) \in NW, t \tag{17}$$

The three binary variables (x^r_{ij},$u^s_{ij,t}$ and$\beta^{r,s}_{ij,t}$) control the switching actions. x^r_{ij} represents whether a switch is installed in line (i,j), $u^s_{ij,t}$ represents whether line (i,j) is damaged in scenario s, and $\beta^{r,s}_{ij,t}$ represents whether the switch is closed in scenario s. These three binary variables determine whether the line (i,j) is in or out. The distribution line status based on this concept is shown in Fig. 2. Constraint (10) states that if a tie switch is installed in the first stage, it can be used for network

reconfiguration in the second stage under a certain scenario. Eqs. (11)–(17) enforce the active and reactive power flow limits on the distribution lines based on the functional status of the lines. Constraints (11)–(15) represent the power flow limits at each tie line. Constraints (16) and (17) indicate that if a distribution line fails in an extreme weather event, its power flow will be necessarily zero.

(3) Power flow constraints: DistFlow equations are applied to define power flows in distribution networks. Linearized Distflow equations have been widely used and verified in problems such as DG placement, MEG pre-positioning, service restoration, and distribution system planning [14,16,25–27]. Constraints (18)–(21) present the linearized Distflow equations, which are used in this paper.

$$\sum_{j\rangle i} P^s_{i,j,t} - \sum_{j\langle i} P^s_{j,i,t} = P^{SUB,s}_{r,t} + P^{DG,s}_{d,t} + P^{MEG,s}_{e,t} - (1-\rho^s_{i,t})P^s_{i,t}, \quad \forall i \in N, \forall r \in R, \forall d \in D, \forall e \in E, \forall (i,j) \in B, t \tag{18}$$

$$\sum_{j\rangle i} Q^s_{i,j,t} - \sum_{j\langle i} Q^s_{j,i,t} = Q^{SUB,s}_{r,t} + Q^{DG,s}_{d,t} + Q^{MEG,s}_{e,t} - (1-\rho^s_{i,t})Q^s_{i,t}, \quad \forall i \in N, \forall r \in R, \forall d \in D, \forall e \in E, \forall (i,j) \in B, t \tag{19}$$

$$V^s_{i,t} - \frac{r_{i,j}P^s_{i,j,t} + x_{i,j}Q^s_{i,j,t}}{V_1} - (1-\beta^{r,s}_{i,j,t} + 1 - x^r_{i,j})M \leqslant V^s_{j,t} \leqslant V^s_{i,t} - \frac{r_{i,j}P^s_{i,j,t} + x_{i,j}Q^s_{i,j,t}}{V_1} + (1-\beta^{r,s}_{i,j,t} + 1 - x^r_{i,j})M, \quad \forall (i,j) \in SW, t \tag{20}$$

$$V^s_{i,t} - \frac{r_{i,j}P^s_{i,j,t} + x_{i,j}Q^s_{i,j,t}}{V_1} - u^s_{i,j,t}M \leqslant V^s_{j,t} \leqslant V^s_{i,t} - \frac{r_{i,j}P^s_{i,j,t} + x_{i,j}Q^s_{i,j,t}}{V_1} + u^s_{i,j,t}M, \quad \forall (i,j) \in NW, t \tag{21}$$

Eqs. (18) and (19) represent the active and reactive power balances at each node. In (20) and (21), the big-M approach is used to ensure that the voltages of the two nodes will be independent if the distribution line between them fails.

(4) Radiality constraints: The radiality constraints are described by (22)–(25) based on the spanning tree approach in [22,28].

$$\alpha^s_{i,j,t} + \alpha^s_{j,i,t} - (1-x^r_{i,j})M \leqslant \beta^{r,s}_{i,j,t} \leqslant \alpha^s_{i,j,t} + \alpha^s_{j,i,t} + (1-x^r_{i,j})M, \quad \forall (i,j) \in SW, t \tag{22}$$

$$\alpha^s_{i,j,t} + \alpha^s_{j,i,t} = l - u^s_{i,j,t}, \forall (i,j) \in NW, t \in T \tag{23}$$

$$\sum_{\forall i} \alpha^s_{i,j,t} \leqslant 1, \forall j, t \tag{24}$$

$$\alpha^s_{i,j,t} = 0, \forall i,j \in BS, t \tag{25}$$

The two binary variables $\alpha^s_{i,j,t}$ and $\alpha^s_{j,i,t}$ are introduced to model the spanning tree structure. Constraints (22) and (23) present the relation between the line connection status and the spanning tree variables $\alpha^s_{i,j,t}$ and$\alpha^s_{j,i,t}$. Constraint (22) states that if the distribution line (*i*,*j*) is connected by closing the tie line switch, then either $\alpha^s_{i,j,t}$ or $\alpha^s_{j,i,t}$ must be one. Constraint (23) states that if the distribution line is connected ($u^s_{i,j,t} = 0$), either node *i* is the parent of node j or vice versa. Constraint (24) states that each node has one or no parent node. Constraint (25) shows that the substation node does not have a parent node and it is a root node.

(5) DG capacity limits: Constraints (26) and (27) indicate the active and reactive power limits of the DG at node *d* if it has been added in the first stage.

$$0 \leqslant P^{DG,s}_{d,t} \leqslant x^{dg}_d P^{DGmax}_d, \forall d \in D, t \tag{26}$$

$$0 \leqslant Q^{DG,s}_{d,t} \leqslant x^{dg}_d Q^{DGmax}_d, \forall d \in D, t \tag{27}$$

(6) MEG allocation limits: Eqs. (28) and (29) state that MEG *k* is sent from the depot toward the nodes.

$$\sum_{k\in K} y^s_{p,k,e} \leqslant x_{p,k}, \forall p \in P, \forall e \in E \tag{28}$$

$$\sum_{p\in P}\sum_{k\in K} y^s_{p,k,e} \leqslant 3, \forall e \in E \tag{29}$$

Constraint (28) enforces that, in each scenario, MEG *k* is sent toward one of the nodes from depot *p*. It seems that if the crew teams are well-trained and the MEGs are equipped with the required modules, parallel operation of 3 MEGs is feasible. This feature is expressed by (29).

(7) MEG capacity limits: the active and reactive power outputs of MEG *k* at a candidate node are formulated as follows:

$$0 \leqslant P^{MEG,s}_{e,t} \leqslant \sum_{p\in P}\sum_{k\in K} y^s_{p,k,e} P^{MEGmax}_k, \forall e \in E, t \tag{30}$$

$$0 \leqslant Q^{MEG,s}_{e,t} \leqslant \sum_{p\in P}\sum_{k\in K} y^s_{p,k,e} Q^{MEGmax}_k, \forall e \in E, t \tag{31}$$

(8) Load shedding constraint: the percentage levels of load shedding as a continuous variable are indicated in (32).

$$0 \leqslant \rho^s_{i,t} \leqslant 1, \forall i \in L, t \tag{32}$$

(9) Voltage magnitude constraint: The upper and lower limits of the node voltage magnitude are indicated in constraint (33).

$$(1-\varepsilon)V_1 \leqslant V^s_{i,t} \leqslant (1+\varepsilon)V_1, \forall i \in N, t \tag{33}$$

(10) Substation power injection limits: Equations (34) and (35) define the active and reactive power injected from the substation, respectively.

$$P^{SUB,s}_{r,t} \geqslant 0, \forall r \in R \tag{34}$$

$$Q^{SUB,s}_{r,t} \geqslant 0, \forall r \in R \tag{35}$$

2.3. Normal operation in the second-stage problem

We consider the case when the utility uses DG for reducing the power purchased from the wholesale market during normal operations. Additionally, this option can reduce power losses in normal situations. During normal operation, the objective function of the utility is:

$$min\ NC_w = \sum_{w=1}^{N_w} T_w \left(\sum_{d\in D}\sum_{t\in T} C^{DG}_o P^{DG,w}_{d,t} \Delta t + \sum_{r\in R}\sum_{t\in T} C^{sub} P^{SUB,w}_{r,t} \Delta t \right) \tag{36}$$

Expression (36) minimizes the total operation cost including the cost of DG operation and purchasing power from the upstream grid over a set of normal scenarios. N_w is the number of normal scenarios (this paper considers four scenarios in spring, summer, fall, and winter). The normal operation is constrained as follows:

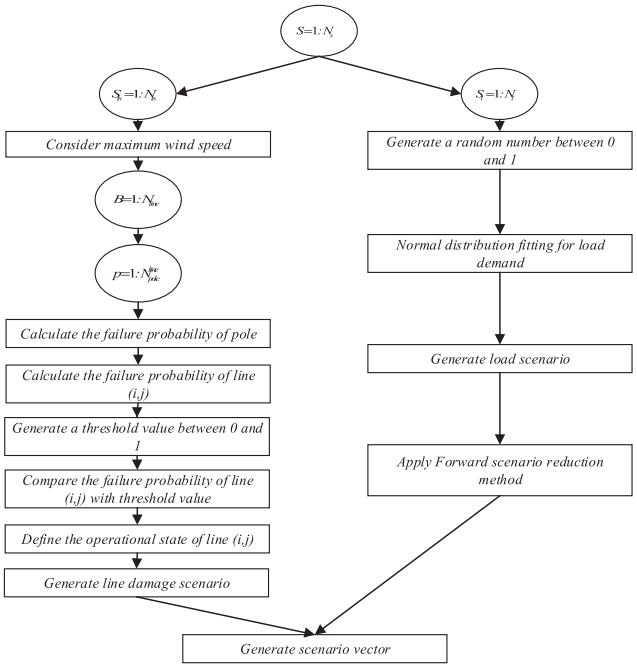

Fig. 3. Flowchart of scenario generation.

$$\sum_{j)i} P^{w}_{i,j,t} - \sum_{j(i} P^{w}_{j,i,t} = P^{SUB,w}_{r,t} + P^{DG,w}_{d,t} - P^{w}_{i,t}, \quad \forall i \in N, \forall r \in R, \forall d \in D, \forall e \in E, \forall (i,j) \in B, t \tag{37}$$

$$\sum_{j)i} Q^{w}_{i,j,t} - \sum_{j(i} Q^{w}_{j,i,t} = Q^{SUB,w}_{r,t} + Q^{DG,w}_{d,t} - Q^{w}_{i,t}, \quad \forall i \in N, \forall r \in R, \forall d \in D, \forall e \in E, \forall (i,j) \in B, t \tag{38}$$

$$-P^{max}_{i,j} \leqslant P^{w}_{i,j,t} \leqslant P^{max}_{i,j}, \forall (i,j) \in NW, t \tag{39}$$

$$-Q^{max}_{i,j} \leqslant Q^{w}_{i,j,t} \leqslant Q^{max}_{i,j}, \forall (i,j) \in NW, t \tag{40}$$

$$V^{w}_{i,t} - \frac{r_{i,j}P^{w}_{i,j,t} + x_{i,j}Q^{w}_{i,j,t}}{V_1} = V^{w}_{j,t}, \forall (i,j) \in NW, t \tag{41}$$

$$\alpha^{w}_{i,j,t} + \alpha^{w}_{j,i,t} = 1, \forall (i,j) \in NW, t \in T \tag{42}$$

$$\sum_{\forall i} \alpha^{w}_{i,j,t} \leqslant 1, \forall j, t \tag{43}$$

$$\alpha^{w}_{i,j,t} = 0, \forall i,j \in BS, t \tag{44}$$

$$0 \leqslant P^{DG,w}_{d,t} \leqslant x^{dg}_{d} P^{DGmax}_{d}, \forall d \in D, t \tag{45}$$

$$0 \leqslant Q^{DG,w}_{d,t} \leqslant x^{dg}_{d} Q^{DGmax}_{d}, \forall d \in D, t \tag{46}$$

$$P^{SUB,w}_{r,t} \geqslant 0, \forall r \in R, t \tag{47}$$

$$Q^{SUB,w}_{r,t} \geqslant 0, \forall r \in R, t \tag{48}$$

$$(1-\varepsilon)V_1 \leqslant V^{w}_{i,t} \leqslant (1+\varepsilon)V_1, \forall i \in N, t \tag{49}$$

Eqs. (37) and (38) represent the active and reactive power balances at each node. Eqs. (39) and (40) enforce the active and reactive power flow limits on the distribution lines. Constraint (41) defines the voltage level at each node. The radiality constraints are indicated by (42)–(44). Eqs. (45) and (46) indicate the active and reactive power limits of DGs. Eqs. (47) and (48) represent the active and reactive power injected from the substation. Finally, constraint (49) limits the nodal voltage magnitude.

2.4. Uncertainty modeling

The uncertainties associated with the line damage status and the electric loads are modeled as follows. The generated scenarios are shown in Fig. 3.

(1) Line damage status: Due to the random nature of extreme weather events, modeling the line damage status is an important issue in resilient distribution system planning. There are two methods to evaluate hurricane risk. The first approach is the probabilistic analysis where historical hurricane records are utilized to develop a probability density function for hurricane parameters. Then, Monte Carlo simulation is applied to simulate future hurricanes, which can be utilized to estimate wind speeds. Based on the above simulation, the wind speed is modeled as a random variable and is integrated with component fragility models to evaluate the risk of components [29]. In the probabilistic method, for each line damage scenario with a different wind speed, the operational state of the distribution line (i,j) is determined. In previous stochastic resilient distribution system planning models, a specific distribution function in the probabilistic method was used to model the wind speed as a random variable [30]. However, due to a lack of sufficient information such as appropriate distribution functions, it is not applicable to generating line damage scenarios based on the different wind speeds.

Therefore, a scenario-based approach is used in which the effect of a certain historical hurricane is investigated rather than the aggregated effect of all possible hurricanes. This means that a selected hurricane level is assumed in the scenario-based method. In addition, the occurrence probability of a hurricane is not needed in this method. Hence, we have utilized the maximum wind speed to model the uncertainty of hurricanes.

After selecting a specified hurricane level, it is necessary to calculate the failure probability of the poles. In this paper, due to the lack of sufficient data for calculating the direct wind-induced failure probability of conductors and the fallen tree-induced failure probability of conductors, we assumed that the failure probability of distribution lines can be extracted by the failure probability of distribution poles. However, if such data become available, the failure probability of distribution lines can be easily derived based on the failure probability of poles and conductors. The failure probability of a distribution pole is calculated by mapping the maximum wind speed with the fragility model of that pole. We assume that failure probabilities of distribution poles are independent and all distribution poles have the same fragility curve. Using the pole fragility model, the failure probability of line (i,j) based on the maximum wind speed can be calculated as follows [31,32]:

$$p_{pole}(w_m) = 0.0001e^{0.0421w_m} \tag{50}$$

$$p_{i,j}(w_m) = 1 - (1 - p_{pole}(w_m))^{N_{pole,i,j}} \tag{51}$$

According to the calculated failure probability of distribution lines, in this paper, we use a threshold method to extract the line damage scenarios based on the failure probability of distribution lines and different vulnerability thresholds as a random variable. The concept of a threshold is usually allied with the concept of resilience in the literature. The importance of thresholds in ecosystem resilience was investigated in [33]. This work used thresholds of disturbance to predict the resilience of an ecosystem in the future. In [34], the concept of thresholds was analyzed for environmental and resilience management. This work used linear and nonlinear regression models to analyze the thresholds. For each line damage scenario with a different threshold, the operational state of each line is obtained by comparing a threshold with the failure

probability of distribution lines. Therefore, in each scenario, distribution line (i,j) is considered out of service ($z^s_{i,j,t} = 1$) if the failure probability exceeds a pre-determined threshold. It is worth mentioning that thresholds can be defined based on the uniform random numbers between 0 and 1 or the experiences of distribution system planners in the face of hurricanes. In the threshold method, it must be noticed that the number of line damage scenarios is proportional to the number of thresholds. Finally, the probability of each line damage scenario is calculated based on the threshold values, as follows:

$$\pi^{TH}_{ts} = \frac{TH_{ts}}{TH_{ts} + \ldots + TH_{N_{ts}}}, \forall ts = 1, \ldots, N_{ts} \quad (52)$$

The procedure of scenario generation for modeling the line damage uncertainty is shown in Algorithm 1. Based on this method, the distribution system planner can overcome the lack of sufficient information and plan accurate designs for the distribution network based on a specific hurricane level.

Algorithm 1 Line damage uncertainty modeling algorithm

1. Start
2. for $s = 1,\ldots,N_{ts}$
3. Consider maximum wind speed.
4. Generate a threshold value (TH_{ts}) based on a uniform distribution.
5. for$(i,j) \in B$
6. Calculate $p_{i,j}(w_m)$via (51).
7. if$p_{i,j}(w_m) \rangle TH_{ts}$
8. $z^s_{i,j,t} = 1$
9. else
10. $z^s_{i,j,t} = 0$
11. end
12. end
13. end
14. Calculate π^{TH}_{ts}via (52).
15. end

(2) Load uncertainty: We consider the uncertainty of load as the "prevailing uncertainty" in the distribution system planning model. In this paper, Monte Carlo simulation is used for generating load scenarios. Then, the scenarios with low probability are merged or removed in a process called scenario reduction. Scenario reduction reduces the computational cost and time of considering all possible scenarios [35]. The Forward Reduction method is utilized in this paper. The procedure of scenario generation for modeling the load uncertainty is shown in Algorithm 2.

Algorithm 2 Load uncertainty modeling algorithm

1. Start
2. Consider t = 1
3. Consider s = 1
4. Generate a random number based on a normal distribution (N(1,0.05))
5. Compute $l_{t,s} = l_{t,0} + \mu_{t,s}\sigma$
6. if all the required scenarios are produced
7. go to line 11
8. else
9. s = s + 1
10. go to line 4
11. if all the required hours are produced
12. go to line 16
13. else
14. t = t + 1
15. go to line 4
16. Save all the produced scenarios
17. end

where $l_{t,0}$ is the predicted hourly load value and σ is the standard deviation of the normal distribution.

(3) Combined line damage-load scenarios: In this study, it is considered that the load and line damage scenarios are independent, and the line damage-load scenarios are combined to make the set of scenarios as follows [30]:

$$\pi_s = \pi^{TH}_{ts} \times \pi_l \quad (53)$$

where $\pi^{TH}_{ts}$and $\pi_l$are the probabilities of the tsth line damage and the lth load scenario, respectively. The total number of emergency scenarios will be $ts \times l$.

2.5. Overview of the proposed approach

Fig. 4 shows the proposed framework for enhancing the distribution system resilience. Prior to solving the MILP model, the two clusters of uncertainties are modeled as a stochastic programming process. Afterward, a set of scenarios representing the realization of stochastic processes are generated. In order to reduce the MILP problem solution time, the number of load scenarios is decreased using the Forward Reduction method. In the subsequent step, the two-stage MILP model is solved using commercially available software packages. The results of the MILP model help the utilities to decide about hardening their networks, installing new back-up DGs, allocating MEGs, and adding automatic tie switches with optimal investment and operation costs.

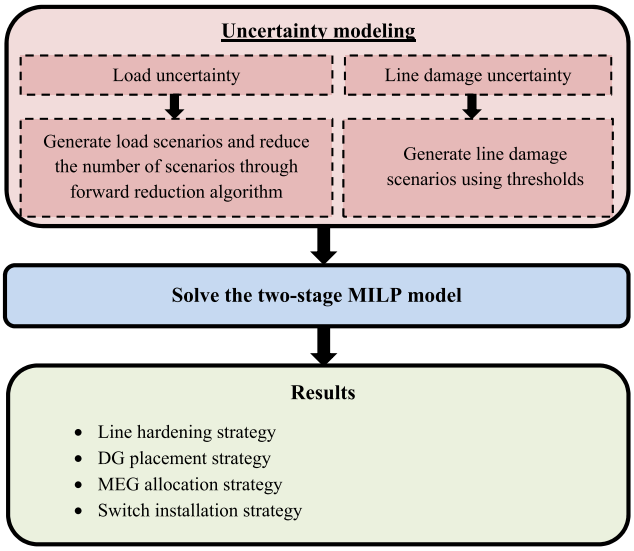

Fig. 4. Framework for resilient distribution system planning.

Table 2
The investment cost of different strategies.

Strategy	Cost ($)
Upgrading poles	6000/pole [5]
Installing a natural gas-fired DG	1000/kW [22]
Allocating a 30 kW MEG	1320$/kW [37]
Allocating a 105 kW MEG	830$/kW [37]
Adding an automatic tie line switch	5000 [22]
Creating a tie-line	10000$/km [38]

3. Case studies

The proposed MILP model is applied to an IEEE 33-node test system and a modified 118-node test system. Similar to the Texas coast [36], we assume the occurrence of one hurricane of category 3 per year. It is supposed that in the worst case, a city close to the coast will be affected

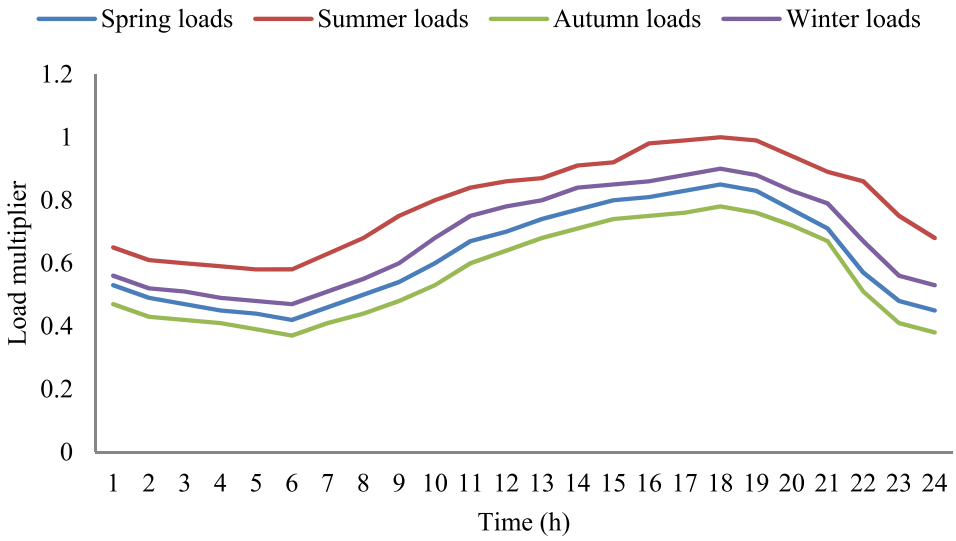

Fig. 5. Multipliers of active and reactive load profiles.

Table 3
The candidate positions for the strategies in the 33-node test system.

Strategy	Candidate positions	Test systems 33 node
Upgrading pole	All line	32
Installing a DG	Pre-selected nodes	2, 4, 8, 11, 18, 21, 22, 24, 25, 26, 30, 33
Allocating a MEG	All nodes	33
Adding a tie line switch	Pre-selected lines	5

Table 4
Number of damaged lines in each scenario in the 33-node test system.

Threshold	Number of damaged lines 33-node
%20	3
%15	8
%10	15

for 24 h. The initial investment cost of resilience improvement strategies is outlined in Table 2. The length of each distribution line is considered to be proportional to its resistance. Therefore, we can estimate the number of distribution poles in each distribution line. Also, we assume that the span between successive distribution poles is 150 ft. The interest rate and the lifetime of the resilience improvement strategies are %10 and 15 years, respectively. The annual investment cost of purchasing and installing each strategy is one-tenth of the initial investment cost.

We assume that there are 5 load priorities with priority values equal to 1, 1.2, 1.4, 1.6, and 2. The basic load shedding cost is considered to be 14 $/kWh [21], and the parameter of load shedding cost in the second stage objective function is the product of the load priority and the basic load shedding cost. Also, the period is considered to be 1 h. The multipliers, shown in Fig. 5, are used to produce the active load profiles in four seasons. The multipliers of the active load profile on a typical day in the summer can be found in [39]. Also, we consider that the multipliers of all buses are the same. In this paper, four normal scenarios are set, each with a duration of 91 days. The cost of purchasing power from the upstream grid is 110 $/MWh. Also, the DG operating cost is 75 $/MWh [40]. The upper and lower limits of voltage magnitude are taken to be 1.05 and 0.95 pu, respectively.

Our program was executed on a PC with an Intel Core i7 CPU @3.20 GHz and 32-GB RAM. The proposed MILP model was solved using the CPLEX solver under the general algebraic modeling system (GAMS) optimization package with a 0.01% optimality gap.

3.1. IEEE 33-node distribution system

This distribution network is supplied by the upstream grid at one point of common coupling and hosts natural gas-fired DGs with 400 kW capacities, which can be controlled by utilities for improving the distribution network resilience. Due to the budget restriction, the total number of candidate DGs is restricted to 4. In addition, we use MEG with 30 kW capacity. We consider that, in this test system, the utility has one depot for crew teams, and the depot can accommodate two MEGs. Also, we consider that 1 crew team is needed for operating each MEG in the distribution network. The total number of MEGs is limited to 2. The candidate positions for various strategies are given in Table 3. The complete node and line data can be found in [7,41].

The line damage scenarios of the 33-node distribution network are extracted subject to the failure probability of the distribution lines and different thresholds. At first, the failure probabilities of distribution lines are calculated according to the fragility function of the poles and lines [32] and the maximum wind speed of the category-3 hurricane [36]. Then, three vulnerability thresholds of %10, %15, and %20 are generated, and the lines with failure probabilities higher than these thresholds are designated as out of service. Based on this method, 3 scenarios for the line damage status are generated. Table 4 presents the number of damaged lines in each scenario. Subsequently, 1000 load scenarios are initially produced using a normal probability density function, and then they are reduced using the Forward Reduction method to 2 scenarios with 2 corresponding probabilities. As stated, the line damage uncertainty and load uncertainty scenarios are combined. Therefore, 6 scenarios are defined for the model.

In the following, four distinct cases are studied to illustrate the effectiveness of the proposed model.

- Case 1: Multi-objective and excluding the reconfiguration capability.
- Case 2: Multi-objective and including the reconfiguration capability.
- Case 3: Single-objective and excluding the reconfiguration capability.
- Case 4: Single-objective and including the reconfiguration capability.

Case 1: In this case, the weighting coefficients are the same, which means that the objective function of normal operation is as important as that of emergency operation. In this case, the optimal resilient

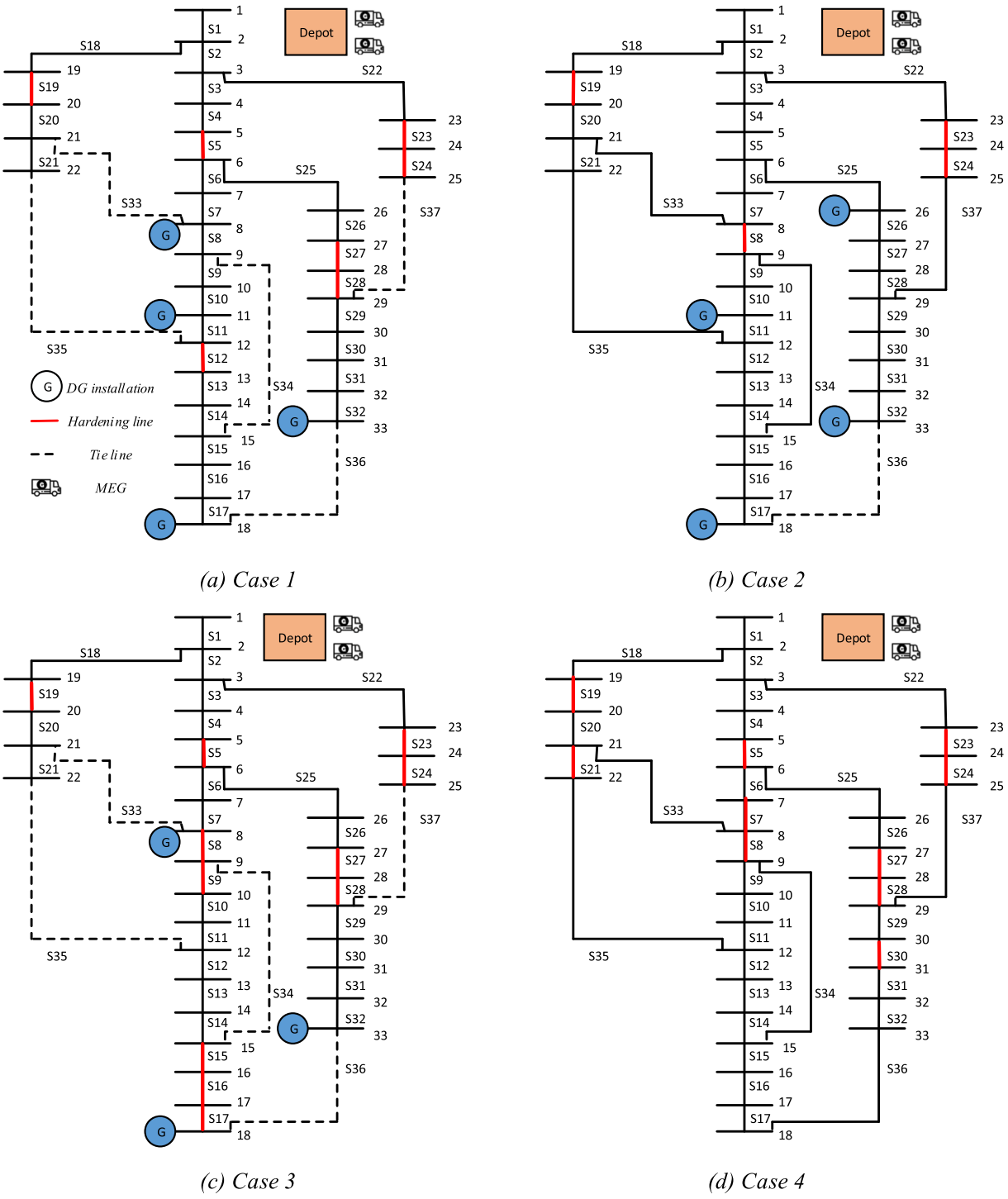

Fig. 6. The optimal investment schemes in the 33-node test system.

distribution system plan is created for the state without reconfiguration during normal and emergency conditions. Fig. 6a depicts the investment scheme without reconfiguration. It should be mentioned that, in Fig. 6a, without reconfiguration means that the distribution network has its initial topology. The value of the objective function with reconfiguration is presented in Table 5. It is worth mentioning that, in this table, the total emergency operation costs are equivalent to the total load shedding costs. As can be seen from Fig. 6a, due to a lack of reconfiguration, the number of hardened lines has been increased for supplying the load points from the upstream network. Additionally, we have four new DGs, which are installed near the load point with high priority.

Case 2: This section intends to provide the optimal investment scheme for the state with reconfiguration during normal and emergency conditions. The planning results with reconfiguration are shown in Fig. 6b. This figure shows the hardening lines, the optimal DG locations, the network topology, and the required number of MEGs. Table 5 indicates the values of investment and operation costs. As shown, considering tie-lines as resilience-oriented design options can significantly reduce the total cost of investment, especially the hardening cost. In fact, the reduction in the line hardening cost due to the installation of tie switches is equal to the reduction in the cost of load shedding, such that line hardening and load shedding cost reductions are approximately

Table 5
Simulation results of the 33-node distribution network.

	33-node system			
	Case 1	Case 2	Case 3	Case 4
Objective function value	1,176,500	1,153,200	222,300	96,418.959
Total investment cost ($)	222,520	205,720	207,720	91,620
Total line hardening cost (S)	54,600	31,800	79,800	76,200
Total normal operation cost ($)	938,968.758	938,968.758	0	0
Total emergency operation cost ($)	15,028.443	8,519.418	14,581.438	4,798.959

Table 6
MEG allocation for different scenarios in the 33 node test system.

Scenarios	MEG Location
S1	MEG 1 allocated to bus 14
S2	MEG 2 allocated to bus 13 MEG 1 allocated to bus 17
S3	MEG 2 allocated to bus 17 MEG 1 allocated to bus 17
S4	MEG 2 allocated to bus 16 MEG 1 allocated to bus 13
S5	MEG 2 allocated to bus 16 MEG 1 allocated to bus 17
S6	MEG 2 allocated to bus 17 MEG 1 allocated to bus 17
	MEG 2 allocated to bus 16

%41 and %43, respectively.

In addition, the impact of the threshold on reductions in the total investment cost and the total load shedding cost is investigated in the 33-node distribution system. For this purpose, we have increased the thresholds by %5. The results indicate that the investment cost and the load shedding cost are 199,120 $ and 2712.884 $, respectively. As predicted, since the numbers of damaged lines are decreased in this case, the total investment cost is lower than the total cost of the previous scenario. Therefore, a compromise should be made between the investment cost and the threshold level in line damage modeling. In this study, the threshold values were assumed to be %10, %15, and %20, which seems rational since both the investment cost and the number of damaged lines are taken into account.

Case 3: In this case, the weighting coefficient of the normal operation objective function is set to zero. The planning results of this case are presented in Table 5. As shown in this table, since the normal operation cost in this case is not considered as one of the operation objectives, the total investment cost is lower than the total investment cost in the corresponding state in case 1. Fig. 6c shows the optimal investment decisions for this state. Due to the lack of tie-line utilization, the optimal planning scheme in this case leads to the allocation of three back-up DGs in the distribution network. As can be seen, almost all of the DGs are allocated in the lower section of the distribution network to compensate for the voltage drop resulting from power transmission.

Case 4: This section was specially designed to illustrate the joint impacts of line hardening, DG installation, MEG allocation, and topology reconfiguration on the load shedding cost following a hurricane. The results of this case, shown in Table 5, indicate that considering tie switches as resilience-oriented design options leads to a total investment cost reduction of 55%, which is more than the corresponding amount in case 2. In this case, MEG allocation is presented in different scenarios in Table 6. As shown in this table, two MEGs were sent toward the same nodes to operate in parallel in scenarios 2 and 5. Fig. 6d shows the optimal investment decisions for this case. As it can be seen, DG installation is not selected as an option to improve the distribution system resilience. The reason is the lower cost of line hardening and tie switch installation despite DG allocation. It means that when the

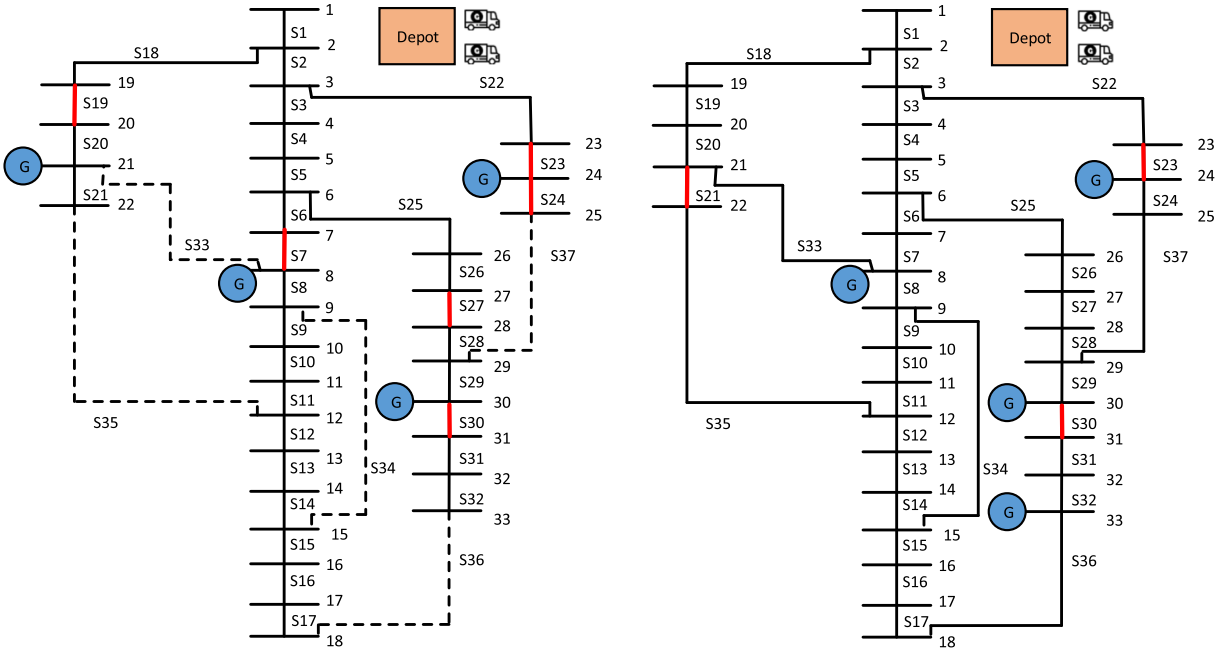

(a) Case 3 *(b) Case 4*

Fig. 7. Optimal investment decisions without an upstream network in the 33-node system.

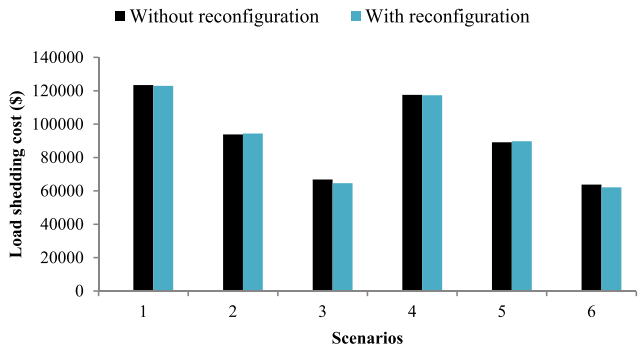

Fig. 8. The load shedding cost ($) under different scenarios in the 33-node system.

Table 7
The candidate positions for the strategies in the 118-node test system.

Strategy	Candidate positions	Test systems 118 node
Upgrading poles	All lines	117
Installing a DG	Pre-selected nodes	7, 17, 24, 33, 37, 43, 51, 59, 66, 74, 80, 84, 96, 103, 107, 111, 114
Allocating a MEG	All nodes	118
Adding a tie line switch	Pre-selected lines	6

Table 8
Number of damaged lines in each scenario in the 118-node test system.

Threshold	Number of damaged lines 118-node
%20	5
%15	12
%10	37

distribution network is supplied by the upstream network, the line hardening strategy is much less expensive than installing a new back-up DG. Therefore, we intend to determine the optimal investment decisions when the distribution network is cut off from the upstream network. The optimal investment decisions for this state are demonstrated in Fig. 7b. The total investment cost of the reconfigured state is $194,620. For the sake of comparison, the load shedding costs during a hurricane for the reconfigured and non-reconfigured states when the upstream network is disconnected are provided in Fig. 8. According to this figure, the load shedding costs in the two states are almost equal. However, the line hardening costs are $51,000 and $19,200 for the non-reconfigured and reconfigured networks, respectively.

3.2. 118-node distribution system

A comprehensive case study of the 118-node test network is performed to validate the application of the proposed model to large systems. This modified 11 kV distribution system has 3 feeders and 118 buses. The total active and reactive demands of this system are 22.71 MW and 17.04 Mvar, respectively. The distribution system possesses natural gas-fired distributed generators, each with 1000 kW capacity. The total number of new DGs is limited to 8. In addition, we use a type of MEG with a 105-kW capacity for the 118-node test system. We assume that the utility has two depots for crew teams, where each depot can accommodate two MEGs. As in the 33-node test system, a crew team is needed for operating each MEG in the distribution network. The total number of MEGs is limited to 4. The candidate positions for various strategies are presented in Table 7. The detailed data about line parameters and system loads can be found in [42,43]. As in the 33-node test system, 3 vulnerability thresholds equal to %10, %15, and %20 are generated, and 3 scenarios are considered for the line outage status. Table 8 presents the number of damaged lines in each scenario for the 118-node test system.

In Fig. 9, the optimal investment strategies of an outage scenario (S2) are shown during an emergency and normal conditions for the 118-node test system. Twelve lines are damaged in this scenario. As depicted in the figure, three lines are hardened and eight back-up DGs and four MEGs are allocated to supply loads. Additionally, three tie switches are installed to make the power flow to the loads. In the 118-node system, different nodes have significantly different loads. For example, an 819-kW demand at priority nodes 50 and 111 must be inevitably supplied, whereas nodes 88 and 117, with respective insignificant load values of 22 and 48 kW, are not powered. It is worth mentioning that the locations of very small loads with high priority may not allow the allocation of a large sum of money to distribution line hardening. For instance, the distribution lines 83–84 and 117–118 are not hardened in order to supply very small priority loads at nodes 84 and 118. However, the required number of MEGs can supply these ignored priority loads. In addition, considering large priority values for these nodes leads to distribution line hardening for supplying these small loads. The optimal investment plan indicates enhanced distribution system resilience as a result of the proposed approach.

The proposed model is compared with each separate scenario in the 118-node distribution system for performance demonstration, as presented in Table 9. As mentioned in the previous section, we consider six scenarios consisting of load and line damage scenarios. In Table 9, it is observed that the objective values in S4, S5, and S6 are much higher than those in the first three scenarios. The reason is the higher load shedding cost in the second three scenarios. However, the first-stage cost reduces significantly if we consider all these scenarios in our model. Consequently, the proposed model can reduce the objective function compared to other distinct scenarios.

4. Conclusions

This paper utilized a threshold method for enhancing the distribution system resilience. The distribution line damage status following a hurricane was considered an uncertain parameter. The presented method deployed different thresholds to decrease the number of line damage scenarios for resilience studies. The proposed two-stage MILP framework was solved using the commercial solver CPLEX under GAMS modeling language. The presented approach was implemented on 33-node and 118-node distribution systems, and the results showed that the optimal line hardening, optimal DG placement, optimal MEG allocation, and optimal tie switch placement can considerably enhance the resilience of distribution networks under emergency conditions. Additionally, the proposed model indicated that topology reconfiguration can significantly decrease economic losses during hurricanes. In the future, we will focus on other resilient distribution network planning resources such as mobile energy storage to form microgrids through the stochastic optimization model.

CRediT authorship contribution statement

Mostafa Ghasemi: Conceptualization, Methodology, Writing - original draft. **Ahad Kazemi:** Supervision, Writing - review & editing. **Ettore Bompard:** Supervision. **Farrokh Aminifar:** Validation, Writing - review & editing.

Declaration of Competing Interest

The authors declare that they have no known competing financial interests or personal relationships that could have appeared to influence the work reported in this paper.

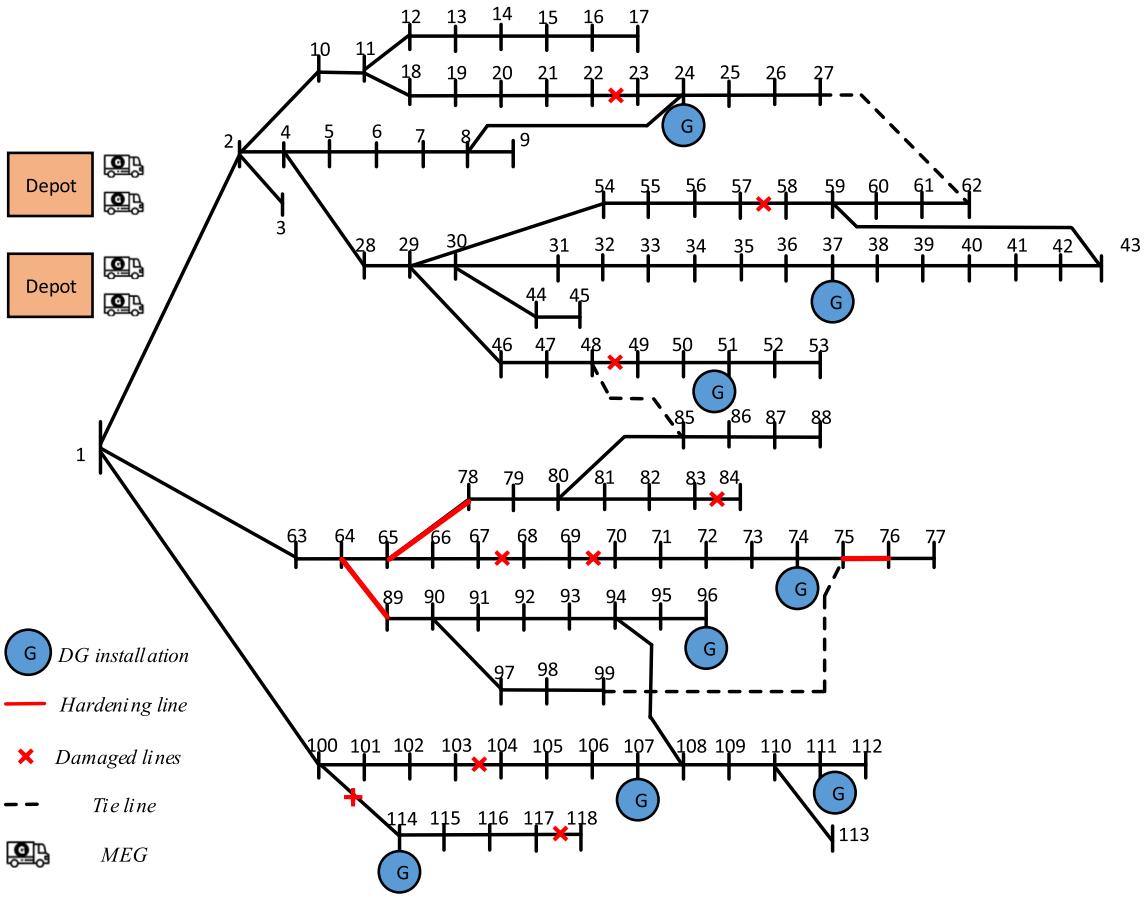

Fig. 9. The optimal investment schemes of an outage scenario in the 118-node test system.

Table 9
Comparison of the proposed model and distinct scenarios.

	Objective value ($)	First stage cost ($)
S1	6,913,579.58	850,460
S2	6,919,227.35	902,360
S3	7,026,183.03	996,560
S4	8,898,482.48	847,860
S5	8,921,144.01	880,760
S6	8,965,347.11	990,560
Proposed model	7,028,000.6	982,460

References

[1] Larsen PH, Lawson M, LaCommare KH, Eto JH. Severe weather, utility spending, and the long-term reliability of the US power system. Energy 2020;14:117387.
[2] Watson EB, Etemadi AH. Modeling electrical grid resilience under hurricane wind conditions with increased solar and wind power generation. IEEE Trans Power Syst 2019.
[3] Gaikwad N, Raman NS, Barooah P. Smart home energy management system for power system resiliency. arXiv preprint arXiv:2003.05570; 2020 Mar 12.
[4] Zare-Bahramabadi M, Abbaspour A, Fotuhi-Firuzabad M, Moeini-Aghtaie M. Resilience-based framework for switch placement problem in power distribution systems. IET Gener Transm Distrib 2017;12(5):1223–30.
[5] Chen B. Applications of optimization under uncertainty methods on power system planning problems; 2016.
[6] Shi Q, Li F, Olama M, Dong J, Xue Y, Starke M, et al. Network reconfiguration and distributed energy resource scheduling for improved distribution system resilience. Int J Electr Power Energy Syst 2021;1(124):106355.
[7] Gilani MA, Kazemi A, Ghasemi M. Distribution system resilience enhancement by microgrid formation considering distributed energy resources. Energy 2020;15 (191):116442.
[8] Amirioun MH, Aminifar F, Lesani H. Resilience-oriented proactive management of microgrids against windstorms. IEEE Trans Power Syst 2017;33(4):4275–84.
[9] Panteli M, Trakas DN, Mancarella P, Hatziargyriou ND. Power systems resilience assessment: hardening and smart operational enhancement strategies. Proc IEEE 2017;105(7):1202–13.
[10] Poudel S, Dubey A. Critical load restoration using distributed energy resources for resilient power distribution system. IEEE Trans Power Syst 2018;34(1):52–63.
[11] Galvan E, Mandal P, Sang Y. Networked microgrids with roof-top solar PV and battery energy storage to improve distribution grids resilience to natural disasters. Int J Electr Power Energy Syst 2020;1(123):106239.
[12] Zhu J, Yuan Y, Wang W. An exact microgrid formation model for load restoration in resilient distribution system. Int J Electr Power Energy Syst 2020;1(116): 105568.
[13] Lei S, Chen C, Li Y, Hou Y. Resilient disaster recovery logistics of distribution systems: co-optimize service restoration with repair crew and mobile power source dispatch. IEEE Trans Smart Grid 2019;10(6):6187–202.
[14] Lei S, Wang J, Chen C, Hou Y. Mobile emergency generator pre-positioning and real-time allocation for resilient response to natural disasters. IEEE Trans Smart Grid 2016;9(3):2030–41.
[15] Yang Z, Dehghanian P, Nazemi M. Enhancing seismic resilience of electric power distribution systems with mobile power sources. In: 2019 IEEE industry applications society annual meeting. IEEE; 2019. p. 1–7.
[16] Zhang G, Zhang F, Zhang X, Wu Q, Meng K. A multi-disaster-scenario distributionally robust planning model for enhancing the resilience of distribution systems. Int J Electr Power Energy Syst 2020;1(122):106161.
[17] Ma S, Chen B, Wang Z. Resilience enhancement strategy for distribution systems under extreme weather events. IEEE Trans Smart Grid 2016;9(2):1442–51.
[18] Wang X, Li Z, Shahidehpour M, Jiang C. Robust line hardening strategies for improving the resilience of distribution systems with variable renewable resources. IEEE Trans Sustain Energy 2017;10(1):386–95.
[19] Aldarajee AH, Hosseinian SH, Vahidi B, Dehghan S. A coordinated planner-disaster-risk-averse-planner investment model for enhancing the resilience of integrated electric power and natural gas networks. Int J Electr Power Energy Syst 2020;1(119):105948.
[20] Yamangil E, Bent R, Backhaus S. Resilient upgrade of electrical distribution grids. In: Twenty-ninth AAAI conference on artificial intelligence; 2015 Feb 16.
[21] Ma S, Su L, Wang Z, Qiu F, Guo G. Resilience enhancement of distribution grids against extreme weather events. IEEE Trans Power Syst 2018;33(5):4842–53.
[22] Ma S, Li S, Wang Z, Qiu F. Resilience-oriented design of distribution systems. IEEE Trans Power Syst 2019;34(4):2880–91.

[23] Najafi J, Peiravi A, Guerrero JM. Power distribution system improvement planning under hurricanes based on a new resilience index. Sustain Cities Soc 2018;1(39):592–604.
[24] Dehghani NL, Darestani YM, Shafieezadeh A. Optimal life-cycle resilience enhancement of aging power distribution systems: a MINLP-based preventive maintenance planning. IEEE Access 2020;8:22324–34.
[25] Baran ME, Wu FF. Network reconfiguration in distribution systems for loss reduction and load balancing. IEEE Power Eng Rev 1989;9(4):101–2.
[26] Chen C, Wang J, Qiu F, Zhao D. Resilient distribution system by microgrids formation after natural disasters. IEEE Trans Smart Grid 2015;7(2):958–66.
[27] Wang Z, Chen B, Wang J, Kim J, Begovic MM. Robust optimization based optimal DG placement in microgrids. IEEE Trans Smart Grid 2014;5(5):2173–82.
[28] Jabr RA, Singh R, Pal BC. Minimum loss network reconfiguration using mixed-integer convex programming. IEEE Trans Power Syst 2012;27(2):1106–15.
[29] Salman AM, Li Y, Stewart MG. Evaluating system reliability and targeted hardening strategies of power distribution systems subjected to hurricanes. Reliab Eng Syst Saf 2015;1(144):319–33.
[30] Nikkhah S, Jalilpoor K, Kianmehr E, Gharehpetian GB. Optimal wind turbine allocation and network reconfiguration for enhancing resiliency of system after major faults caused by natural disaster considering uncertainty. IET Renew Power Gener 2018;12(12):1413–23.
[31] Ouyang M, Duenas-Osorio L. Multi-dimensional hurricane resilience assessment of electric power systems. Struct Saf 2014;1(48):15–24.
[32] Amirioun MH, Aminifar F, Lesani H. Towards proactive scheduling of microgrids against extreme floods. IEEE Trans Smart Grid 2017;9(4):3900–2.
[33] Standish RJ, Hobbs RJ, Mayfield MM, Bestelmeyer BT, Suding KN, Battaglia LL, et al. Resilience in ecology: abstraction, distraction, or where the action is? Biol Conserv 2014;1(177):43–51.
[34] Li Y, Li Y, Wu W. Threshold and resilience management of coupled urbanization and water environmental system in the rapidly changing coastal region. Environ Pollut 2016;1(208):87–95.
[35] Imani MH, Niknejad P, Barzegaran MR. Implementing Time-of-Use Demand Response Program in microgrid considering energy storage unit participation and different capacities of installed wind power. Electr Power Syst Res 2019;1(175):105916.
[36] Brown RE. Cost-benefit analysis of the deployment of utility infrastructure upgrades and storm hardening programs. Raleigh: Quanta Technology; 2009.
[37] Zhou B, Xu D, Li C, Cao Y, Chan KW, Xu Y, et al. Multiobjective generation portfolio of hybrid energy generating station for mobile emergency power supplies. IEEE Trans Smart Grid 2017;9(6):5786–97.
[38] Hoseinpour M, Haghifam MR, Zangiabadi M, Larimi SM. Simultaneous optimisation of tie switches placement and reserve capacity margin of sub-transmission substations considering the conflict between short-term and long-term plannings. CIRED-Open Access Proc J 2017;2017(1):2534–8.
[39] Wang Z, Wang J. Self-healing resilient distribution systems based on sectionalization into microgrids. IEEE Trans Power Syst 2015;30(6):3139–49.
[40] Wong S, Bhattacharya K, Fuller JD. Electric power distribution system design and planning in a deregulated environment. IET Gener Transm Distrib 2009;3(12):1061–78.
[41] Abessi A, Zakariazadeh A, Vahidinasab V, Ghazizadeh MS, Mehran K. End-user participation in a collaborative distributed voltage control and demand response programme. IET Gener Transm Distrib 2018;12(12):3079–85.
[42] Ali ES, Abd Elazim SM, Abdelaziz AY. Improved Harmony Algorithm for optimal locations and sizing of capacitors in radial distribution systems. Int J Electr Power Energy Syst 2016;1(79):275–84.
[43] Geng L, Lu Z, He L, Zhang J, Li X, Guo X. Smart charging management system for electric vehicles in coupled transportation and power distribution systems. Energy 2019;15(189):116275.